

## A COMPARATIVE STUDY OF PENTAQUARK INTERPOLATING CURRENTS

R.D. Matheus, F.S. Navarra, M. Nielsen, R. Rodrigues da Silva

*Instituto de Física, Universidade de São Paulo**C.P. 66318, 05315-970 São Paulo, SP, Brazil*

## Abstract

In a diquark-diquark-antiquark picture of pentaquarks, we use two interpolating currents to calculate the mass of the recently measured  $\Xi^{--}$  state in the framework of QCD sum rules. We show that, even though yielding similar values for  $m_{\Xi^{--}}$  (and close to the experimental value), these currents differ from each other in what concerns the strength of the pole, convergence of the OPE and sensitivity to the continuum threshold parameter.

## I. INTRODUCTION

After the recent discovery of pentaquark states [1, 2, 3, 4, 5] the central question to be addressed now concerns the structure of these new baryons. They could be: a) uncorrelated quarks inside a bag [6]; b) a  $K - N$  molecule bound by a van-der Waals force [7]; c) a “ $K - N$ ” bound state in which  $uud$  and  $u\bar{s}$  are not separately in color singlet states [8]; d) a diquark-triquark  $(ud) - (ud\bar{s})$  bound state [9] and e) a diquark-diquark-antiquark (DDA) state. This last one was advanced by Jaffe and Wilczek (JW) [10] and is quite appealing because it can explain two unusual features of pentaquarks: their small mass and decay width. Instantons generate strong attractive quark-quark interactions with the formation of low mass diquarks, which, in turn, lead to relatively low mass pentaquarks. This was verified in [11], [12] and [13]. Moreover, in [14], it was shown that the DDA configuration may lead to strongly suppressed transition amplitudes (to meson-baryon states) for a reasonable choice of its spatial wave function, namely, two separated extended diquark balls overlapping only partially and the antiquark at the center of the system.

Pentaquark configurations can be implemented in QCD sum rules (QCDSR) [15, 16] and in lattice QCD [17, 18] by a proper choice of the interpolating current. A current for configuration c) has been proposed by Zhu [8] and for configuration e) three different currents were proposed in [11], [12] and [13].

Given the impulse of this field and the prospects of new measurements, we may expect that the “pentaquark wave” will last still for a long time. A great effort will be devoted to understand the structure of these objects. For the QCDSR community (and for lattice QCD studies as well) this means that more attention will have to be given to the properties of the interpolating currents. At this point, we can already compare the three calculations presented in [11], [12] and [13] for the mass of the  $\Theta^+$ . Although they present different implementations of the DDA scheme, they produce very similar results for the pentaquark mass. This indicates that a more careful analysis has to be performed.

The purpose of the present work is twofold. We will use QCDSR to calculate the mass of the recently measured  $\Xi^{--}$  and we will also take the opportunity to perform a careful comparison of the results obtained with two different currents, which we will call I and II. Current I was introduced by us in [11] and current II is the one proposed in [12]. As it will be seen, both currents give approximately the same mass for the  $\Xi^{--}$  but have different sensi-

tivity to the continuum threshold parameter, different convergence of the operator product expansion (OPE) and also different strength of the pole, with respect to the continuum. This comparative study, which will later be extended to the currents suggested in [13] and also in [19], will give us a better understanding of these currents and may lead to the choice of the best current.

## II. CURRENTS AND CORRELATION FUNCTIONS

In the QCDSR approach [15, 16], the short range perturbative QCD is extended by an OPE expansion of the correlators, which results in a series in powers of the squared momentum with Wilson coefficients. The convergence at low momentum is improved by using a Borel transform. The expansion involves universal quark and gluon condensates. The quark-based calculation of a given correlator is equated to the same correlator, calculated using hadronic degrees of freedom via a dispersion relation, providing sum rules from which a hadronic quantity can be estimated. The QCDSR calculation of hadronic masses centers around the two-point correlation function given by

$$\Pi(q) \equiv i \int d^4x e^{iq \cdot x} \langle 0 | T\eta(x)\bar{\eta}(0) | 0 \rangle , \quad (1)$$

where  $\eta(x)$  is an interpolating field (a current) with the quantum numbers of the hadron we want to study.

### A. Current I

Following the diquark-diquark-antiquark scheme, we can write two independent interpolating fields with the quantum numbers of  $\Xi^{--}$ :

$$\eta_1(x) = \frac{1}{\sqrt{2}} \epsilon_{abc} (d_a^T(x) C \gamma_5 s_b(x)) [d_c^T(x) C \gamma_5 s_e(x) + s_e^T(x) C \gamma_5 d_c(x)] C \bar{u}_e^T(x) \quad (2)$$

$$\eta_2(x) = \frac{1}{\sqrt{2}} \epsilon_{abc} (d_a^T(x) C s_b(x)) [d_c^T(x) C s_e(x) + s_e^T(x) C d_c(x)] C \bar{u}_e^T(x) \quad (3)$$

where  $a, b, c$  and  $e$  are color index and  $C = -C^T$  is the charge conjugation operator.

As in the nucleon case, where one also has two independent currents with the nucleon quantum numbers [20, 21], the most general current for  $\Xi^{--}$  is a linear combination of the currents given above:

$$\eta(x) = [t\eta_1(x) + \eta_2(x)] , \quad (4)$$

with  $t$  being an arbitrary parameter. In the case of the nucleon, the interpolating field with  $t = -1$  is known as Ioffe's current [20]. With this choice for  $t$ , this current maximizes the overlap with the nucleon as compared with the excited states, and minimizes the contribution of higher dimension condensates. In the present case it is not clear a priori which is the best choice for  $t$ . This will be studied in what follows.

## B. Current II

We also employ the following interpolating field operator for the pentaquark  $\Xi^{--}$  [12, 18]

:

$$\eta(x) = \epsilon^{abc} \epsilon^{def} \epsilon^{cfg} \{s_a^T(x) C d_b(x)\} \{s_d^T(x) C \gamma_5 d_e(x)\} C \bar{u}_g^T(x) \quad (5)$$

It is easy to confirm that this operator produces a baryon with  $J = 1/2$ ,  $I = 3/2$  and strangeness  $-2$ . The parts,  $S^c(x) = \epsilon^{abc} s_a^T(x) C \gamma_5 d_b(x)$  and  $P^c(x) = \epsilon^{abc} s_a^T(x) C d_b(x)$ , give the scalar  $S$  ( $0^+$ ) and the pseudoscalar  $P$  ( $0^-$ )  $sd$  diquarks, respectively. They both belong to the anti-triplet representation of the color SU(3). The scalar diquark corresponds to the the  $I = 1/2$   $sd$  quark with zero angular momentum. It is known that a gluon exchange force as well as the instanton mediated force commonly used in the quark model spectroscopy give significant attraction between the quarks in this channel.

## C. Mass sum rules for the $\Xi^{--}$

Inserting Eq. (4) into the integrand of Eq. (1) we obtain

$$\langle 0 | T\eta(x) \bar{\eta}(0) | 0 \rangle = t^2 \Pi_{11}(x) + t (\Pi_{12}(x) + \Pi_{21}(x)) + \Pi_{22}(x) \quad (6)$$

Calling  $\Gamma_1 = \gamma_5$  and  $\Gamma_2 = 1$  we get

$$\begin{aligned} \Pi_{ij}(x) = \langle 0 | T\eta_i(x) \bar{\eta}_j(0) | 0 \rangle &= \epsilon_{abc} \epsilon_{a'b'c'} C S_{e'e}^T(-x) C \left\{ - \text{Tr} [\Gamma_i S_{bb'}^s(x) \Gamma_j C S_{aa'}^T(x) C] \right. \\ &\times \text{Tr} [\Gamma_i S_{ee'}^s(x) \Gamma_j C S_{cc'}^T(x) C] + \text{Tr} [\Gamma_i S_{be'}^s(x) \Gamma_j C S_{cc'}^T(x) C \Gamma_i S_{eb'}^s(x) \Gamma_j C S_{aa'}^T(x) C] \\ &+ \text{Tr} [\Gamma_i S_{bb'}^s(x) \Gamma_j C S_{ca'}^T(x) C \Gamma_i S_{ee'}^s(x) \Gamma_j C S_{ac'}^T(x) C] - \text{Tr} [\Gamma_i S_{be'}^s(x) \Gamma_j C S_{ac'}^T(x) C] \\ &\times \text{Tr} [\Gamma_i S_{eb'}^s(x) \Gamma_j C S_{ca'}^T(x) C] - \text{Tr} [\Gamma_i S_{ab'}(x) \Gamma_j C S_{ea'}^{sT}(x) C \Gamma_i S_{ce'}^s(x) \Gamma_j C S_{bc'}^{sT}(x) C] \\ &- \text{Tr} [\Gamma_i S_{ba'}^s(x) \Gamma_j C S_{cb'}^T(x) C \Gamma_i S_{ec'}^s(x) \Gamma_j C S_{ae'}^T(x) C] + \text{Tr} [\Gamma_i S_{ba'}^s(x) \Gamma_j C S_{ab'}^T(x) C] \\ &\times \text{Tr} [\Gamma_i S_{ce'}^s(x) \Gamma_j C S_{ec'}^{sT}(x) C] + \text{Tr} [\Gamma_i S_{bc'}^s(x) \Gamma_j C S_{ae'}^T(x) C] \text{Tr} [\Gamma_i S_{ea'}^s(x) \Gamma_j C S_{cb'}^T(x) C] \left. \right\}, \quad (7) \end{aligned}$$

where  $S_{ab}(x)$  and  $S_{ab}^s(x)$  are the light and strange quark propagators respectively.

In order to evaluate the correlation function  $\Pi(q)$  at the quark level, we first need to determine the quark propagator in the presence of quark and gluon condensates. Keeping track of the terms linear in the quark mass and taking into account quark and gluon condensates, we get [22]

$$\begin{aligned} S_{ab}(x) = \langle 0 | T[q_a(x)\bar{q}_b(0)] | 0 \rangle &= \frac{i\delta_{ab}}{2\pi^2 x^4} \not{x} - \frac{m_q \delta_{ab}}{4\pi^2 x^2} - \frac{i}{32\pi^2 x^2} t_{ab}^A g_s G_{\mu\nu}^A (\not{x}\sigma^{\mu\nu} + \sigma^{\mu\nu} \not{x}) \\ &- \frac{\delta_{ab}}{12} \langle \bar{q}q \rangle - \frac{m_q}{32\pi^2} t_{ab}^A g_s G_{\mu\nu}^A \sigma^{\mu\nu} \ln(-x^2) + \frac{i\delta_{ab}}{48} m_q \langle \bar{q}q \rangle \not{x} - \frac{x^2 \delta_{ab}}{2^6 \times 3} \langle g_s \bar{q} \sigma \cdot \mathcal{G} q \rangle \\ &+ \frac{ix^2 \delta_{ab}}{2^7 \times 3^2} m_q \langle g_s \bar{q} \sigma \cdot \mathcal{G} q \rangle \not{x} - \frac{x^4 \delta_{ab}}{2^{10} \times 3^3} \langle \bar{q}q \rangle \langle g_s^2 G^2 \rangle, \end{aligned} \quad (8)$$

where we have used the factorization approximation for the multi-quark condensates, and we have used the fixed-point gauge [22].

Inserting (8) into (7) we obtain a set of diagrams which contribute to the OPE side of the correlation function. In the case of the current I, Fig. 1 shows the classes of diagrams which we are considering. In each diagram, except the perturbative one, all possible permutations of the lines are implicit.

Lorentz covariance, parity and time reversal imply that the two-point correlation function in Eq. (1) has the form

$$\Pi(q) = \Pi_1(q^2) + \Pi_q(q^2) \not{q}. \quad (9)$$

A sum rule for each scalar invariant function  $\Pi_1$  and  $\Pi_q$ , can be obtained. As in ref. [8], in this work we shall use the chirality even structure  $\Pi_q(q^2)$  to obtain the final results but we shall also discuss the chirality odd structure  $\Pi_1$ , showing its limitations for our present purposes.

The phenomenological side is described, as usual, as a sum of pole and continuum, the latter being approximated by the OPE spectral density. In order to suppress the condensates of higher dimension and at the same time reduce the influence of higher resonances we perform a standard Borel transform [15]:

$$\Pi(M^2) \equiv \lim_{n, Q^2 \rightarrow \infty} \frac{1}{n!} (Q^2)^{n+1} \left( -\frac{d}{dQ^2} \right)^n \Pi(Q^2) \quad (10)$$

( $Q^2 = -q^2$ ) with the squared Borel mass scale  $M^2 = Q^2/n$  kept fixed in the limit.

For current II we repeat the steps mentioned above, substituting (5) into (1), making use of the expansion (8), picking up the terms multiplying the structure  $\not{q}$  and finally performing

a Borel transform (10). In this case the diagrams that have to be considered are shown in Fig. 2.

After Borel transforming each side of  $\Pi_q(Q^2)$  and transferring the continuum contribution to the OPE side we obtain the following sum rule at order  $m_s$ :

$$\lambda_{\Xi}^2 e^{-\frac{m_{\Xi}^2}{M^2}} = \int_0^{s_0} e^{-\frac{s}{M^2}} \rho_i^q(s) ds. \quad (11)$$

where  $i (= I, II)$  refers to the current employed and the spectral densities, up to order 6 are given by:

$$\begin{aligned} \rho_I^q(s) = & c_1 \frac{s^5}{5!5!2^{12}7\pi^8} + c_3 \frac{s^3}{5!2^{10}\pi^6} m_s \langle \bar{s}s \rangle - c_4 \frac{s^3}{5!2^8\pi^6} m_s \langle \bar{q}q \rangle \\ & + c_2 \frac{s^3}{5!3!2^{13}\pi^6} \langle \frac{\alpha_s}{\pi} G^2 \rangle + 7c_4 \frac{s^2}{2^{16}\pi^6} m_s \langle \bar{q}g_s \sigma \cdot \mathbf{G} q \rangle \\ & + c_2 \frac{s^2}{3^2 2^{11}\pi^4} \left( \langle \bar{s}s \rangle^2 + \langle \bar{q}q \rangle^2 \right) + c_4 \frac{s^2}{3!2^8\pi^4} \langle \bar{s}s \rangle \langle \bar{q}q \rangle \\ & - c_5 \frac{s^2}{4!3!2^{11}\pi^6} m_s \langle \bar{s}g_s \sigma \cdot \mathbf{G} s \rangle \\ & - 3c_4 \frac{s^2}{4!3!2^{12}\pi^6} m_s \langle \bar{q}g_s \sigma \cdot \mathbf{G} q \rangle \left( 6 \ln\left(\frac{s}{\Lambda_{QCD}^2}\right) - \frac{43}{2} \right), \end{aligned} \quad (12)$$

with  $c_1 = 5t^2 + 2t + 5$ ,  $c_2 = (1-t)^2$ ,  $c_3 = (t+1)^2$ ,  $c_4 = t^2 - 1$ ,  $c_5 = t^2 + 22t + 1$ ,  $\Lambda_{QCD} = 110$  MeV and

$$\begin{aligned} \rho_{II}^q(s) = & \frac{s^5}{5!5!2^{10}7\pi^8} + \frac{s^3}{5!3!2^7\pi^6} m_s \langle \bar{s}s \rangle + \frac{s^3}{5!3!2^{10}\pi^6} \langle \frac{\alpha_s}{\pi} G^2 \rangle \\ & + \frac{s^2}{4!3!2^9\pi^6} m_s \langle \bar{s}g_s \sigma \cdot \mathbf{G} s \rangle. \end{aligned} \quad (13)$$

To extract the  $\Xi^{--}$  mass,  $m_{\Xi}$ , we take the derivative of Eq. (14) with respect to  $M^{-2}$  and divide it by Eq. (14). Repeating the same steps leading to (14), (12) and (13) for the chirality odd structure  $\Pi_1(q^2)$  we arrive at

$$\lambda_{\Xi}^2 m_{\Xi} e^{-\frac{m_{\Xi}^2}{M^2}} = \int_0^{s_0} e^{-\frac{s}{M^2}} \rho_i^1(s) ds. \quad (14)$$

where

$$\rho_I^1(s) = -c_1 \frac{s^4}{5!4!2^{10}\pi^6} \langle \bar{q}q \rangle + c_1 \frac{s^3}{4!3!2^{12}\pi^6} \langle \bar{q}g_s \sigma \cdot \mathbf{G} q \rangle \quad (15)$$

and

$$\rho_{II}^1(s) = -\frac{s^4}{5!4!2^7\pi^6} \langle \bar{q}q \rangle + \frac{s^3}{4!3!2^9\pi^6} \langle \bar{q}g_s \sigma \cdot \mathbf{G} q \rangle \quad (16)$$

In the complete theory, the mass extracted from the sum rule should be independent of the Borel mass  $M^2$ . However, in a truncated treatment there will always be some dependence left. Therefore, one has to work in a region where the approximations made are supposedly acceptable and where the result depends only moderately on the Borel variables.

### III. EVALUATION OF THE SUM RULES AND RESULTS

Before proceeding with the numerical analysis, a remark is in order. A comparison between results obtained with different currents is more meaningful when they describe the same physical state, i.e., those with the same quantum numbers. Concerning spin, all currents considered in our work have the same spin ( $= 1/2$ ). Concerning the parity, the situation is more complicated. In QCD sum rules, when we construct the current, it has a definite parity. Current I has parity  $P = -1$  and current II has parity  $P = +1$ . However, currents can couple to physical states of different parities. As well discussed in [23], in order to know the parity of the state in QCDSR, we have to analyze the chiral-odd sum rule. If the r.h.s of this sum rule (containing the spectral density coming from QCD) is positive, then the parity of the corresponding physical state is the same as the parity of the current. If it is negative the parity is the opposite of the parity of the current. Performing this analysis we might determine in both cases the parity of the state. However it turns out that for both currents, in the chiral-odd sum rule the OPE does not have good convergence, i.e., terms containing higher order operators are not suppressed with respect to the lowest order ones. This sum rule is thus ill defined and nothing can be said about the parity of the state. The comparative study of the currents is still valid because we can compare other properties of these currents. A possible outcome of this study might be that one current has defects, which are so severe that we are forced to abandon it. If this turns out to be case, the determination of the parity of the associated states becomes irrelevant.

Having presented the main formulas in the last section, the next step will be to introduce numerical values for the masses and condensates, choose reasonable values for the free (or partially constrained) parameters, which are the continuum threshold, the Borel mass at which the mass sum rule is evaluated and, in the case of current I, the value of  $t$ . As a result we obtain values for  $m_{\Xi}$ . In doing these calculations we must remember that *it is not enough to obtain a pentaquark mass consistent with the experimental number*. There is a list

of requirements that must be fulfilled:

- i) the physical observables, such as masses and coupling constants, must be approximately independent of the Borel mass (this is the so called Borel stability).
- ii) the right hand side (RHS) of the sum rule (14) must be positive, since the left hand side (LHS) is manifestly positive.
- iii) the operator product expansion (OPE) must be convergent, i.e., the terms appearing in (12) and (13) must decrease with the increasing order of the operator.
- iv) the pole contribution must be dominant, i.e., the integral in (14) must be at least 50 % of the integral over the complete domain of invariant masses ( $s_0 \rightarrow \infty$ ).
- v) the threshold parameter  $s_0$  must be compatible with the energy corresponding to the first excitation of an usual baryon.
- vi) the current-state overlap  $\lambda_{\Xi}$  must be sizeable. The larger is  $\lambda_{\Xi}$  the better is the current.

As it will be seen the above conditions are not easy to be simultaneously satisfied and may be useful in discriminating between different currents.

In the numerical analysis of the sum rules, the values used for the condensates are:  $\langle \bar{q}q \rangle = -(0.23)^3 \text{ GeV}^3$ ,  $\langle \bar{s}s \rangle = 0.8 \langle \bar{q}q \rangle$ ,  $\langle \bar{s}g_s \sigma \cdot \mathbf{G} s \rangle = m_0^2 \langle \bar{s}s \rangle$  with  $m_0^2 = 0.8 \text{ GeV}^2$  and  $\langle g_s^2 G^2 \rangle = 0.5 \text{ GeV}^4$ . We define the continuum threshold as:

$$s_0 = (1.86 + \Delta)^2 \text{ GeV}^2 \quad (17)$$

### A. current I

We evaluate our sum rules in the range  $1.0 \leq M^2 \leq 4.0 \text{ GeV}^2$ . The results are shown in Table I. The first column in Table I gives the values of  $t$  considered here. We notice that some values were excluded, as for example  $t = 0$ , because they would lead to a violation of condition ii) above. The symbol S stands for a current composed by scalar diquarks only, i.e.,  $\eta_1$ . The motivation for studying this current is to verify if it gives a smaller mass for the pentaquark than those obtained with other currents. According to the instanton description of diquark dynamics, this should be the case. In the second and third columns of Table I we list the values adopted for the strange quark mass and continuum threshold respectively. The fourth column shows  $m_{\Xi}$  and the Borel mass squared at which the particle mass was extracted. The fifth and sixth columns show the ratios of terms containing dimension 4 (quark and gluon condensates) and 6 (mixed condensates) operators and the perturbative

term respectively. Ideally these numbers should be smaller than one, the second being smaller than the first. Finally, the last column shows the strength of the pole. In practice this quantity is obtained dividing the integral in the right hand side of (14) by the same integral with the upper limit  $s_0 = \infty$ . This percentage must be as large as possible, but usually we accept values around 50 %.

As it can be seen in Table I, it is hard to satisfy conditions i) - vi) simultaneously. In particular, when we have a very good OPE convergence, the strength of the pole is very weak and vice versa. We have to look for a compromise and we believe that the choices indicated in bold face are the best. For same choices for  $m_s$  and  $\Delta$  we observe that the masses found with scalar diquark currents,  $S$ , are only slightly smaller than the others. This means either that instanton dynamics was not captured by our choice of currents and diagrams or that the interaction between the pseudoscalar diquarks (included in the mixed currents) is more attractive than expected. The connection between our approach and instantons deserves further investigation.

In order to further illustrate these results, we consider the parameters of the first line in bold face,  $m_s = 0.10$  GeV and  $\Delta = 0.44$  GeV, and construct, Figures 3, 4 and 5, showing the Borel mass dependence of  $m_{\Xi}$ , of the OPE terms (in absolute value) and of the percentage of the pole contribution respectively. For these choices the value of the current-state overlap is:

$$\lambda_I^q \simeq 5.4 \times 10^{-9} \text{ GeV}^{13} \quad (18)$$

In view of the variety of results presented in Table I and in the figures, it would be somewhat artificial to invent a procedure to determine the average value of the  $\Xi$  mass and its corresponding error. If we simply take the average over all values presented we arrive at:

$$m_{\Xi} = 1.87 \pm 0.22 \text{ GeV} \quad (19)$$

Restricting ourselves to the parameter combinations which satisfy the requirements i) - vi) and taking the average we obtain:

$$m_{\Xi} = 1.85 \pm 0.05 \text{ GeV} \quad (20)$$

These numbers are very close to the experimental value.

## B. current II

Using the same numerical inputs quoted in the last subsection we evaluate now the sum rules obtained with current II. The results are shown in Table II, which has the same format as Table I except for the fact that, now, there is no  $t$  parameter. The same comments made for the results of Table I apply here. Choosing the parameters of the first line in bold face,  $m_s = 0.10$  GeV and  $\Delta = 0.24$  GeV, we present in Figures 6, 7 and 8 the Borel mass dependence of  $m_{\Xi}$ , of the OPE terms and of the percentage of the pole respectively. As it can be seen, with current II we tend to overestimate  $m_{\Xi}$ , unless very low threshold parameters or quark masses are used. Besides, the pole contribution is always smaller than 40 %. On the other hand, the Borel stability seen in Fig. 6 is remarkable. This suggests that we could choose a lower value for the Borel mass, thereby increasing the pole contribution without significantly changing  $m_{\Xi}$ . In order to extract from Table II some value for the pentaquark mass, we repeat the procedure applied in the last subsection. The simple average gives:

$$m_{\Xi} = 2.00 \pm 0.16 \text{ GeV} \quad (21)$$

and the average over the best parameter choices leads to:

$$m_{\Xi} = 1.88 \pm 0.04 \text{ GeV} \quad (22)$$

These numbers are somewhat high but still compatible with data. Finally, for these parameters the current-state overlap is:

$$\lambda_I^q \simeq 1.3 \times 10^{-9} \text{ GeV}^{13} \quad (23)$$

Comparing (18) and (23) we observe that the coupling of current I to the the  $\Xi$  state is four times larger than the coupling of current II to this state. This speaks in favor of current I.

## IV. SUMMARY AND CONCLUSIONS

In conclusion, we have presented a QCD sum rule study of the  $\Xi^{--}$  pentaquark mass using a diquark-diquark-antiquark scheme. We have employed two possible currents (I and II) which implement this picture. Several parameter choices were considered for the currents.

We could conclude that for both currents it was possible to find a set of parameters and a Borel window so that conditions i) - vi) were fulfilled and a reasonable value for the mass was found. The ratio pole/total, presented in the tables is still small and probably is the most important drawback of the studied currents.

At the present stage we may say that the pentaquark  $\Xi^{--}$  can be reasonably well described by QCD sum rules and the value of its mass is given by (20) or by (22). These numbers can be considered the same within the uncertainties. Concerning the currents, there are differences in the Borel stability, in the sensitivity to the strange quark mass, in the continuum threshold and in the their couplings to the  $\Xi$  state.

Acknowledgements: We are indebted to S. Narison for fruitful discussions. This work has been supported by CNPq and FAPESP (Brazil).

---

- [1] T. Nakano *et al.*, LEPS Coll., Phys. Rev. Lett. **91**, 012002 (2003).
- [2] V. Barmin *et al.*, DIANA Coll., Phys. Atom. Nucl. **66**, 1715 (2003).
- [3] S. Stepanyan *et al.*, CLAS Coll., Phys. Rev. Lett. **91**, 252001 (2003).
- [4] J. Barth *et al.*, SAPHIR Coll., hep-ex/0307083.
- [5] NA49 Collaboration, C. Alt *et al.*, Phys. Rev. Lett. **92**, 042003 (2004).
- [6] D. Strotman, Phys. Rev. **D20**, 748 (1979).
- [7] This configuration was considered in the case of a  $uudcc\bar{c}$  state in: S.J. Brodsky, I. Schmidt, G.F. de Teramond, Phys. Rev. Lett. **64**, 1011 (1990).
- [8] S.-L. Zhu, Phys. Rev. Lett. **91**, 232002 (2003).
- [9] M. Karliner and H. Lipkin, hep-ph/0307243.
- [10] R. Jaffe and F. Wilczek, Phys. Rev. Lett. **91**, 232003 (2003).
- [11] R.D. Matheus, F.S. Navarra, M. Nielsen, R. Rodrigues da Silva and S.H. Lee, Phys.Lett. **B578**, 323 (2004).
- [12] J. Sugiyama, T. Doi, M. Oka, Phys. Lett. **B581**, 167 (2004).
- [13] M. Eidenmueller, hep-ph/0404126.
- [14] D. Melikhov, S. Simula and B. Stech, hep-ph/0405037.
- [15] M.A. Shifman, A.I. and Vainshtein and V.I. Zakharov, Nucl. Phys. **B147**, 385 (1979).

- [16] L.J. Reinders, H. Rubinste in and S. Yazaki, Phys. Rep. **127**, 1 (1985).
- [17] F. Csikor *et al.*, JHEP 0311, 70 (2003); T.W. Shiu, T.H. Hsieh, hep-ph/0403020; N. Matur *et al.*, hep-ph/0406196.
- [18] S. Sasaki, hep-lat/0310014.
- [19] L. Ya. Glozman, Phys. Lett. **B575**, 18 (2003).
- [20] B. L. Ioffe, Nucl. Phys. **B188**, 317 (1981); **B191**, 591(E) (1981).
- [21] Y. Chung, H. G. Dosch, M. Kremer, D. Schall, Phys. Lett. **B102**, 175 (1981); Nucl. Phys. **B197**, 55 (1982).
- [22] K.-C. Yang *et al.*, Phys. Rev. **D47**, 3001 (1993).
- [23] Hungchong Kim, Su Houng Lee, Phys. Lett. **B595**, 293 (2004).

t	$m_s$ (GeV)	$\Delta$ (GeV)	$m_{\Xi}(M_B^2)$ (GeV)	Dim 4/Pert	Dim 6/Pert	Pole/Total
-1	0.15	0.44	1.95 (3.5)	2.42	3.67	2.1 %
-1	0.15	0.44	1.66 (1.0)	0.36	7.7	80 %
1	0.15	0.44	2.09 (3.5)	0.96	0.53	0.28 %
1	0.15	0.44	1.82 (1.0)	1.44	1.11	40 %
S	0.15	0.44	1.94 (3.5)	2.42	11.6	4.8 %
S	0.15	0.44	1.65 (1.0)	3.62	23.9	87 %
-1	0.12	0.44	1.95 (3.5)	0.24	3.8	2.1 %
-1	0.12	0.44	1.66 (1.0)	0.36	8.0	80 %
1	0.12	0.44	2.09 (3.5)	0.76	0.42	0.32 %
1	0.12	0.44	1.86 (1.0)	1.15	0.89	41 %
S	0.12	0.44	1.94 (3.5)	1.95	11.6	4.8 %
S	0.12	0.44	1.65 (1.0)	2.93	24.1	87 %
-1	0.10	0.44	1.95 (3.5)	0.24	3.89	2.1 %
-1	0.10	0.44	1.66 (1.0)	0.36	8.2	80 %
1	0.10	0.44	2.09 (3.5)	0.64	0.35	0.34 %
<b>1</b>	<b>0.10</b>	<b>0.44</b>	<b>1.88 (1.0)</b>	<b>0.96</b>	<b>0.74</b>	<b>41 %</b>
S	0.10	0.44	1.93 (3.5)	1.64	11.7	4.8 %
S	0.10	0.44	1.64 (1.0)	2.47	24.3	87 %
1	0.09	0.44	2.09 (3.5)	0.57	0.31	0.36 %
<b>1</b>	<b>0.09</b>	<b>0.44</b>	<b>1.90 (1.0)</b>	<b>0.86</b>	<b>0.67</b>	<b>42 %</b>
1	0.09	0.34	2.00 (3.5)	0.68	0.40	0.23 %
1	0.09	0.34	1.81 (1.0)	0.97	0.78	34 %

**Table I:** Results for the  $\Xi^{--}$  obtained with current I.

$m_s$ (GeV)	$\Delta$ (GeV)	$m_{\Xi}(M_B^2)$ (GeV)	Dim 4/Pert	Dim 6 /Pert	Pole/Total (%)
0.15	0.24	2.03 (3.5)	0.02	0.44	0.11 %
0.15	0.44	2.16 (3.5)	0.02	0.26	0.35 %
0.12	0.14	1.88 (3.5)	0.35	0.46	0.10 %
0.12	0.14	1.93 (1.0) <sup>2</sup>	0.46	0.76	16 %
0.10	0.24	1.93 (3.5)	0.47	0.29	0.22 %
<b>0.10</b>	<b>0.24</b>	<b>1.87 (1.0)<sup>2</sup></b>	<b>0.64</b>	<b>0.52</b>	<b>28.7 %</b>
0.09	0.24	1.84 (1.0) <sup>2</sup>	0.76	0.46	31.1 %
<b>0.09</b>	<b>0.34</b>	<b>1.91 (1.0)<sup>2</sup></b>	<b>0.67</b>	<b>0.39</b>	<b>39.0 %</b>

**Table II:** Results for the  $\Xi^{--}$  obtained with current II.

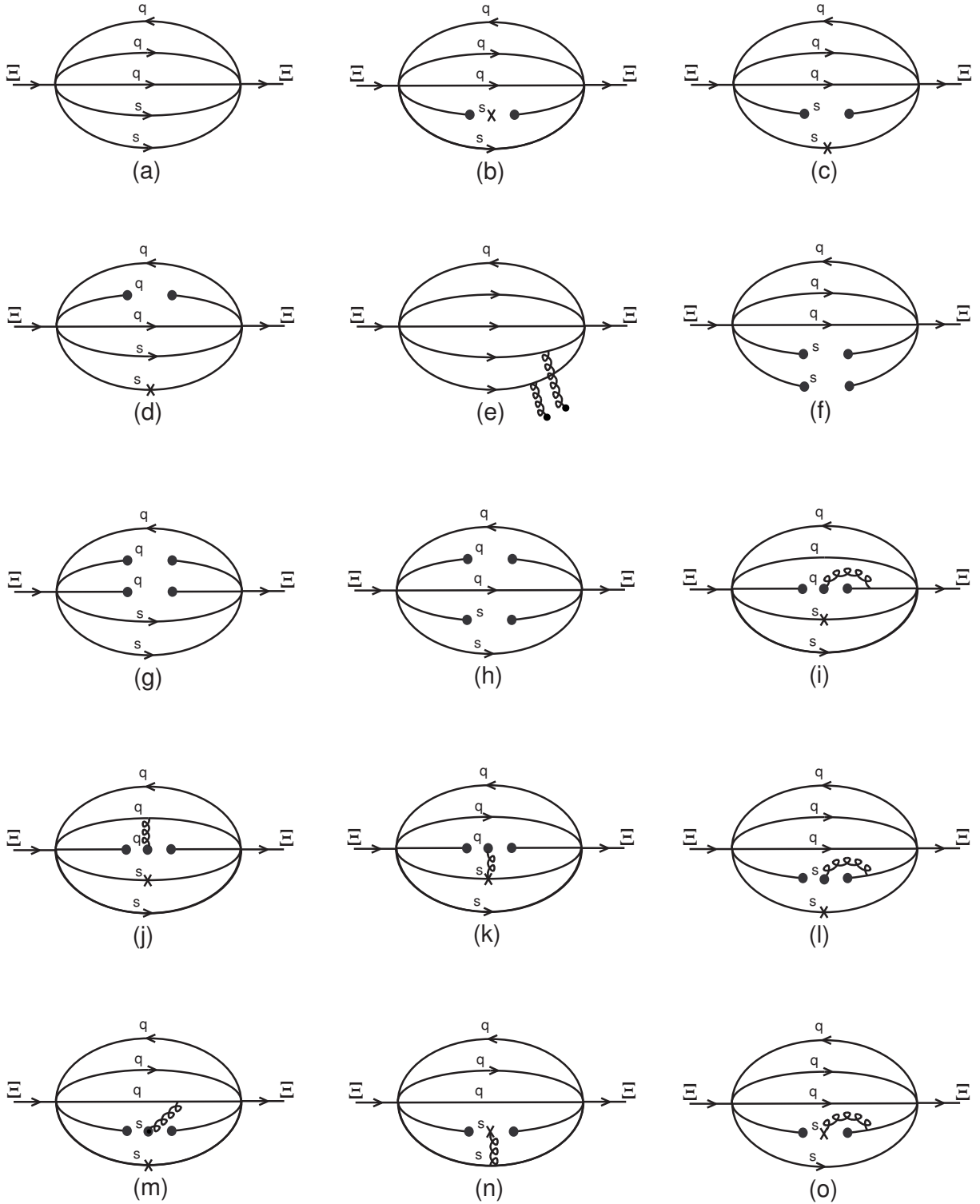


FIG. 1: Classes of diagrams which contribute to the OPE of current  $I$  up to dimension 6: a) perturbative; b)-d) quark condensate; e) gluon condensate; f)-h) 4-quark condensate; i)-o) mixed condensate.

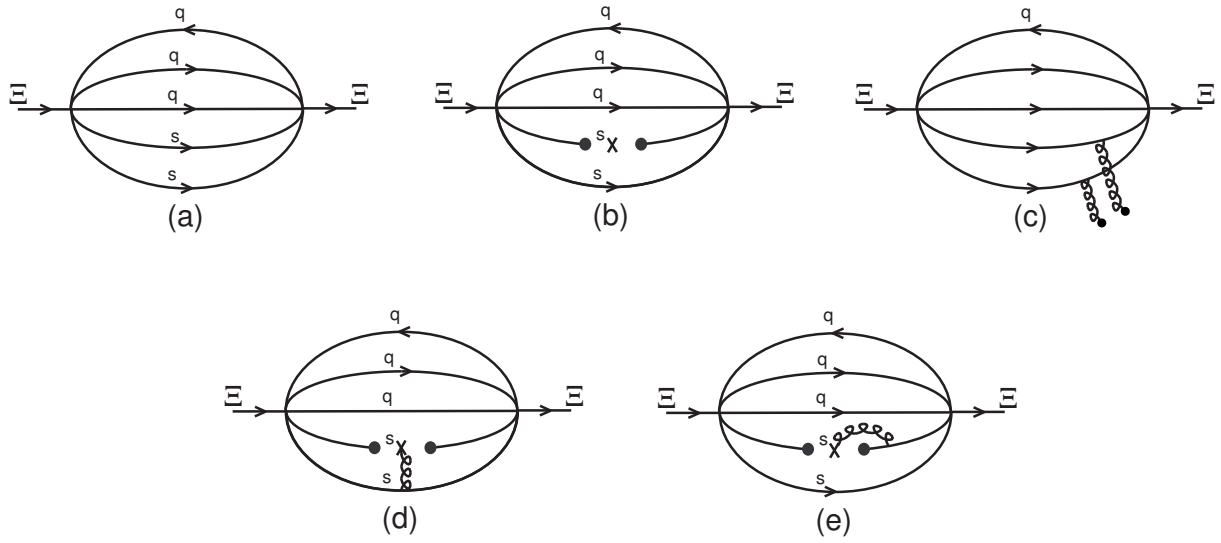


FIG. 2: Diagrams which contribute to the OPE of current II: a) perturbative; b) quark condensate; c) gluon condensate; d)-e) mixed condensate.

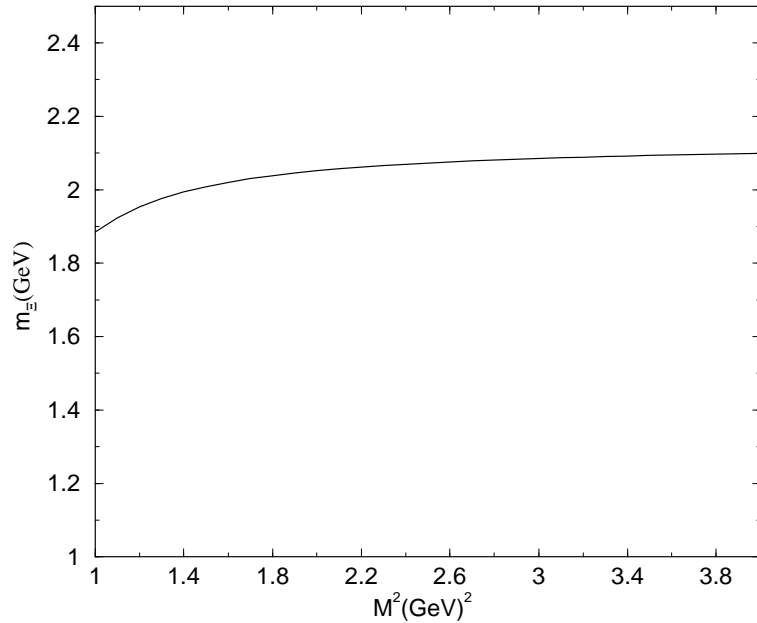


FIG. 3:  $\Xi$  mass with current I.  $m_s = 0.10 \text{ GeV}$ ,  $t = 1$  and  $\Delta = 0.44 \text{ GeV}$ .

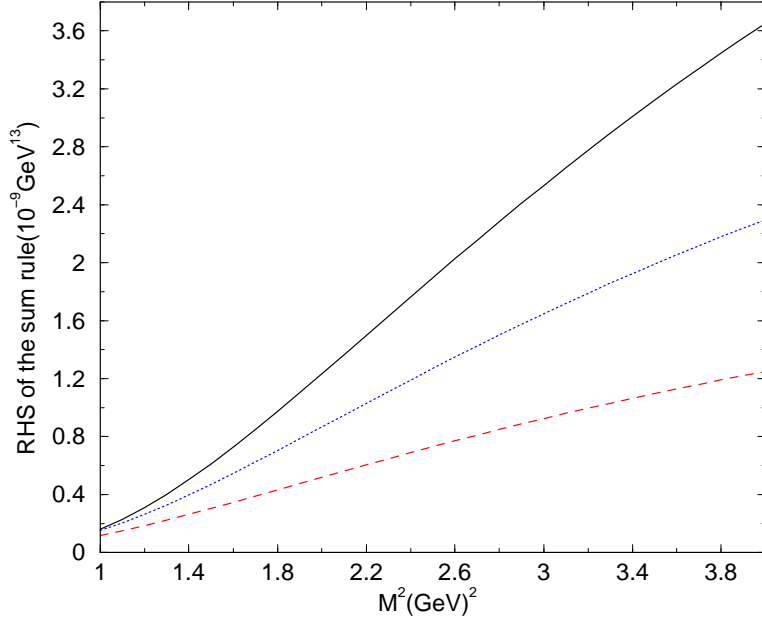


FIG. 4: Leading terms of the R.H.S of (14) with current I.  $m_s = 0.10 \text{ GeV}$ ,  $t = 1$  and  $\Delta = 0.44 \text{ GeV}$ . Solid line: perturbative term; dotted line: operators of dimension 4; dashed line: operators of dimension 6.

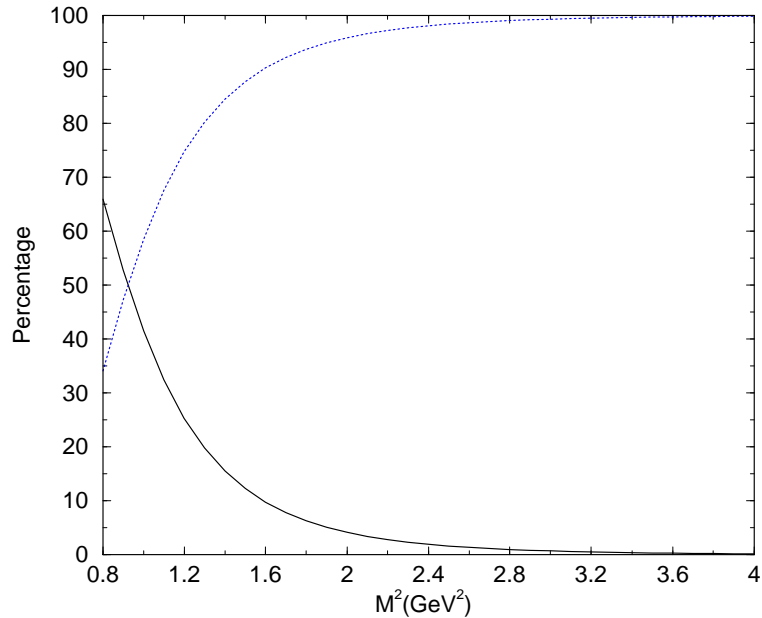


FIG. 5: Relative strength of the pole (solid line) and the continuum (dotted line) as a function of the Borel mass squared with current I.  $m_s = 0.10 \text{ GeV}$ ,  $t = 1$  and  $\Delta = 0.44 \text{ GeV}$ .

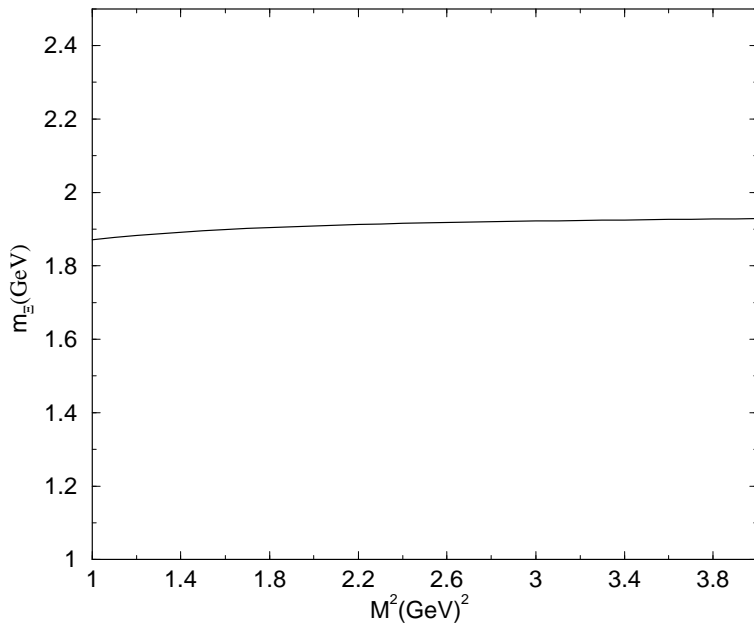


FIG. 6:  $\Xi$  mass with current II.  $m_s = 0.10 \text{ GeV}$  and  $\Delta = 0.24 \text{ GeV}$ .

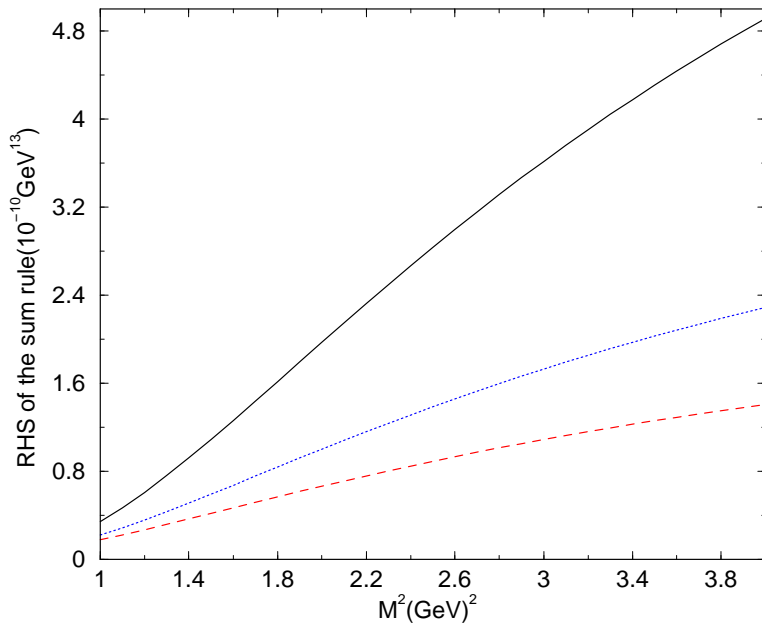


FIG. 7: Leading terms of the R.H.S of (14) with current II.  $m_s = 0.10 \text{ GeV}$  and  $\Delta = 0.24 \text{ GeV}$ . Solid line: perturbative term; dotted line: operators of dimension 4; dashed line: operators of dimension 6.

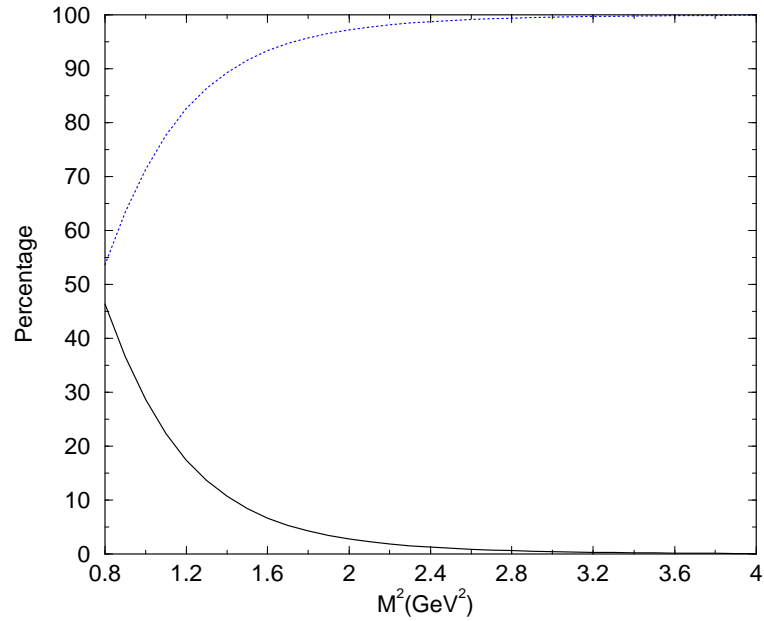


FIG. 8: Relative strength of the pole (solid line) and the continuum (dotted line) as a function of the Borel mass squared with current II.  $m_s = 0.10 \text{ GeV}$ ,  $t = 1$  and  $\Delta = 0.24 \text{ GeV}$ .